

Material and structural testing to improve composite tidal turbine blade reliability

P. Davies, N. Dumergue, M. Arhant, E. Nicolas, S. Paboeuf, P. Mayorga

Abstract— Most tidal turbine blades are currently made from glass or carbon fibre reinforced epoxy composites. These represent a significant part of the turbine cost, but few data are available either to validate current safety factors or to propose alternative more environmentally-friendly materials. This study, performed within the EU H2020 RealTide project, aimed to provide these data. First, a detailed investigation of the static and fatigue behavior was performed at the coupon scale, including not only those materials currently used, but also alternative recyclable thermoplastic matrix composites and natural fibre reinforced materials. Tests were performed before and after seawater saturation, in order to quantify the change in design properties with water uptake. Then a first full scale 5 meter long composite blade was designed and tested to failure. A specific test frame was built, allowing loads up to 75 tons to be applied and simulating the applied moments corresponding to service loads. Static and cyclic loads were applied and extensive instrumentation was used to detect changes in behavior, including optical fibres implanted during manufacture, acoustic emission recording, and specific instrumentation developed within the project. The results have enabled numerical simulations to be verified, and this has provided confidence in the modelling tools. These were then employed in order to propose an improved design of a lower cost blade.

Keywords— Composite blade, Durability, Full scale test.

I. INTRODUCTION

Fibre reinforced composites are widely used in marine applications and in wind turbines but the development of tidal turbines has introduced new,

Manuscript received 15 December, 2021; published 10 June, 2022. This open access article is distributed under the terms of the Creative Commons Attribution 4.0 licence (CC BY <http://creativecommons.org/licenses/by/4.0/>). This work was supported by the EU under Horizon2020 grant GA 727689.

This article has been subject to single-blind peer review by a minimum of two reviewers.

P. Davies, N. Dumergue and M. Arhant work at the French Ocean Research Institute, IFREMER, Centre Bretagne 29280 Plouzané, France (e-mail: peter.davies@ifremer.fr).

E. Nicolas works at Sabella, 7, rue Félix Le Dantec, 29000 Quimper, France (e.nicolas@sabella.bzh).

S. Paboeuf is at Bureau Veritas Marine & Offshore, 4 rue Duguay, Trouin 44800 Saint Herblain, France (stephane.paboeuf@bureauveritas.com).

P. Mayorga is at EnerOcean SL, Bulevar Louis Pasteur 5, Of.321, 29010 Málaga, Spain (Pedro.mayorga@enerocean.com).

more severe constraints. The blades for these devices require complex hydrodynamic shapes, excellent mechanical behaviour under much higher loads than wind blades of similar power output (as bending moments are similar but tidal blades are much shorter), and long term durability in seawater. In addition, designers must also consider environmental factors such as microplastic generation and end of life disposal, so that material selection is a complex optimization process.

These considerations were examined in the EU RealTide project (2018-2021) which is addressing all aspects of the reliability of tidal turbines [1]. In this paper the focus is on the evaluation of alternative materials and improved understanding of blade behaviour. The latter has been investigated through the development of a full scale blade test.

II. MATERIALS

Within the project a range of materials has been tested under static and cyclic loading, both unaged and after seawater saturation. Table 1 presents the materials studied.

TABLE I
MATERIALS STUDIED

Material	Characteristics
Glass/Epoxy	Reference Glass composite
Glass/Polypropylene	Recyclable Glass composite
Carbon/Epoxy	Reference Carbon composite
C/PA6	Recyclable Carbon composite
C/Green epoxy	Partly biosourced matrix
Flax/Acrylic	Natural fibre, recyclable matrix

Carbon is the most widely-used fibre reinforcement for tidal turbine blades today, so that is the reference material here.

Three carbon fibre reinforced materials were studied:

- a reference carbon/epoxy produced by infusion under vacuum, which was tested with different reinforcement stacking sequences (0° , 90° , $\pm 45^\circ$, $0/90^\circ$, $0/\pm 45^\circ$),
- a similar carbon reinforced system but with low pressure manufacture and a partially bio-sourced (green) epoxy matrix,
- a carbon fibre reinforced polyamide 6 material, manufactured from prepreg by hot compression moulding.

Glass reinforced composites have been used in some turbines and there is some debate over the need to use carbon fibre reinforcement [2], so two glass fibre composites were investigated:

- a reference E-glass/epoxy produced by infusion under vacuum, which was tested with different reinforcement stacking sequences (0° , 90° , $\pm 45^\circ$, $0/90^\circ$, $0/\pm 45^\circ$),
- a glass reinforced polypropylene manufactured from prepreg by hot compression moulding, with two sequences (0° and $0/90^\circ$).

Finally a more novel material with a lower environmental impact was also tested, to compare with the glass/epoxy reference:

- flax fibre reinforced acrylic. Natural flax fibre reinforcement has been shown to have a lower environmental impact than glass fibre [3] and the fibres were impregnated by vacuum infusion with an acrylic resin, Elium™. This resin has the advantage of being a liquid, so it can be infused at room temperature with traditional boatyard technology, but it becomes a thermoplastic after solidification and the monomer can be recovered at the end of service life. Again, two sequences were studied, 0° and 90° .

III. MATERIAL TESTING METHODS

Initially the quality of test panels was checked by ultrasonic inspection, calorimetry (DSC) to check cure, and interlaminar shear tests (ASTM D 2344).

The mechanical tests which were then performed were of two types:

- Quasi-static tests, tension, in-plane shear, four point flexure, and
- Cyclic loading tests, performed mainly under four point flexure, both on unaged specimens, tested dry in air, and on seawater saturated specimens which were tested immersed in natural seawater.

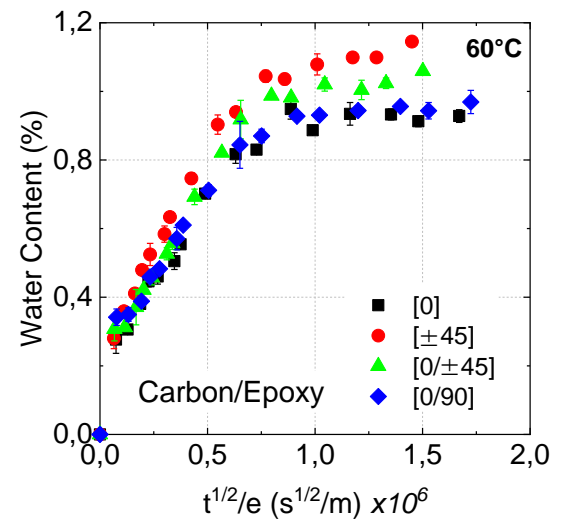
The quasi-static tests followed standard procedures (ASTM 3039, 3518, 790,) with appropriate extensometry. The cyclic flexural tests were performed on 25 kN capacity MTS machines with a sinusoidal load applied at a frequency of 2 Hz and a loading ratio (minimum force/maximum force) $R=0.1$. Specimen loading span was either 100 or 120mm depending on specimen thickness and fibre orientation.

IV. SEAWATER AGING

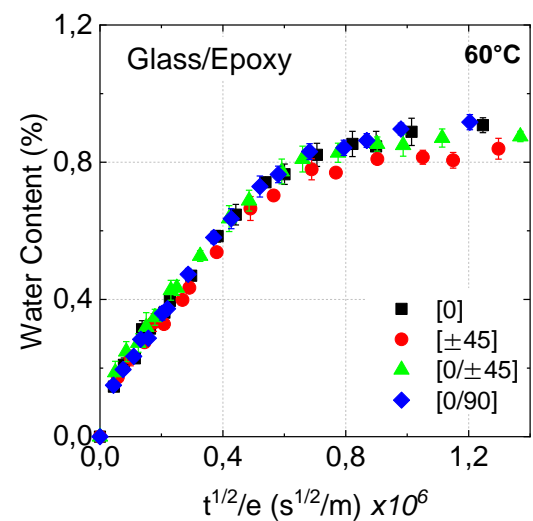
In order to condition samples for testing the accelerated seawater aging facility at IFREMER was employed.

First, seawater diffusion kinetics were quantified by immersing square coupons in water baths at different temperatures. Fig. 1 shows an example of the plots obtained for the two reference materials with different reinforcement orientations. Both material saturate at

around 1% weight gain, with little influence of the fibre orientation. The main parameter in these tests is the matrix content, provided the fibre/matrix interface is good [4]. These materials have the same epoxy matrix and were produced in an identical manner by infusion. These results show that saturation in seawater at 60°C takes about 10 weeks for this sample thickness (2 mm).



(a)



(b)

Fig. 1. Weight gain plots for (a) carbon reinforced and (b) glass reinforced epoxy reference composites. (t : time, e : coupon thickness, s : seconds, m : meters)

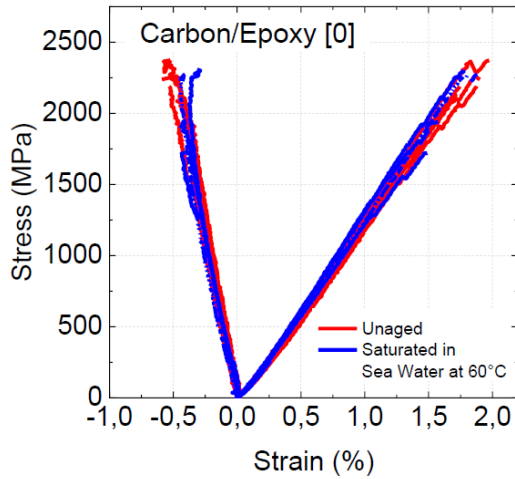
Based on these results, and others at other water temperatures, it was possible to predict the time to saturation of the test specimens with other geometries.

V. MATERIAL COMPARISONS

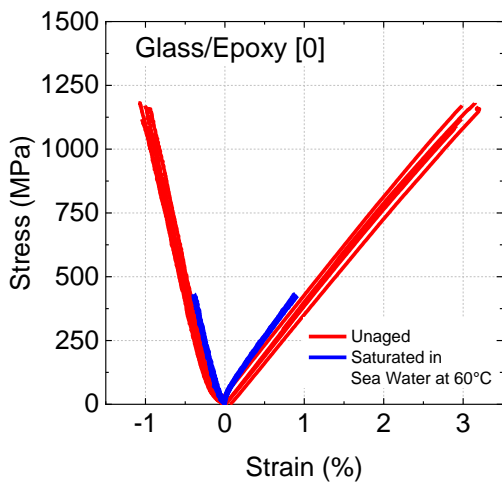
The mechanical test programme involved hundreds of tests, and has generated a large material property database; given the limited space here only some examples will be presented.

The first data needed in design are a set of material stiffnesses, obtained by tensile tests on 0° , 90° and $\pm 45^\circ$

specimens. These are straightforward to measure and for glass and carbon/epoxy composites various published values exist. An example for the two reference materials tested in the fibre direction is shown below, Figure 2. This underlines the excellent property retention in carbon/epoxy but reveals a significant influence of water on the glass/epoxy composite strength (modulus is not affected). Given that the matrix alone is not very sensitive to seawater this indicates an interface degradation mechanism.



(a)



(b)

Fig.2. Test results for 0° specimens (a) C/epoxy and (b) glass/epoxy, loaded along the fibre direction both dry and seawater saturated

However, it is much more difficult to have access to these properties for alternative materials, and it is even rarer to find values to use in design for them after a prolonged period in seawater, so this was one of the first aims of this part of the project. Examples of results from these tests are shown below for carbon/polyamide, glass/PP and flax/acrylic, in the fibre direction for unidirectional specimens in Fig. 3,

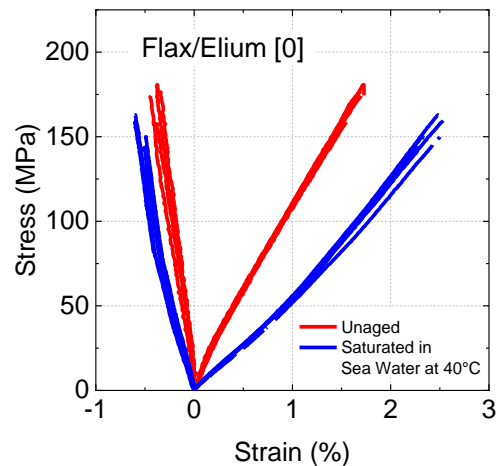
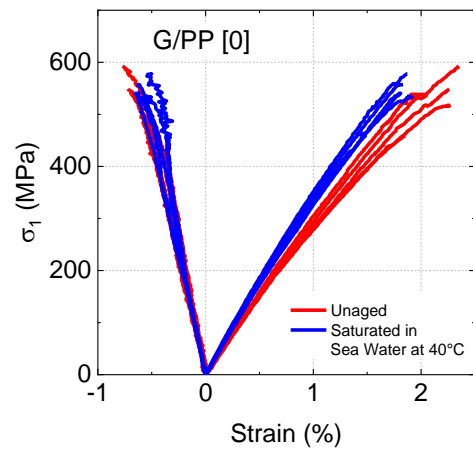
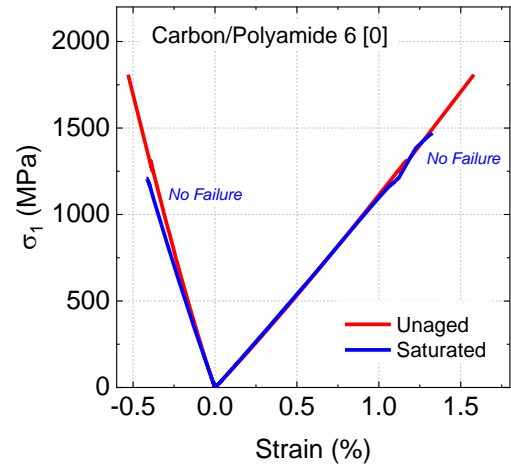


Fig.3. Test results for 0° specimens of three alternative materials, loaded along the fibre direction both dry and seawater saturated.

It is clear that the 0° tensile strength values are lower and that strength retention is more limited for these materials. It is also important to characterize these alternative materials under loads which depend on matrix and interface properties. Once again the carbon reinforced reference material was tested first, Figure 4.

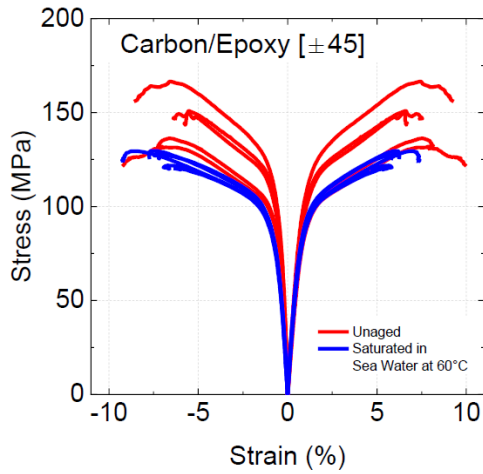


Fig.4. In-plane shear behaviour

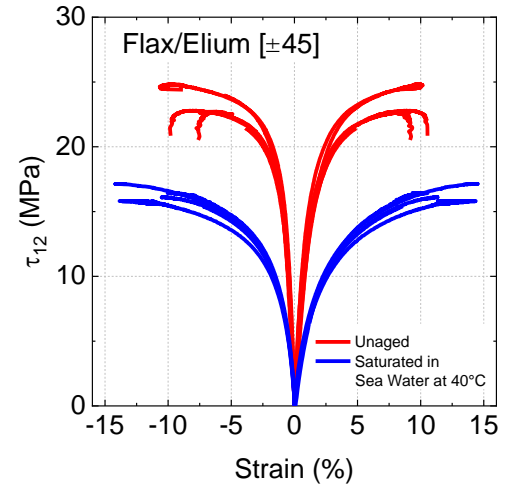


Fig.5. Test results for $\pm 45^\circ$ specimens, tested dry and seawater saturated.

A small drop in shear properties after seawater saturation is noted. Then examples of results are shown for the alternative materials, Figure 5.

Here significant differences are visible for the carbon and flax reinforced composites, the glass/PP is less sensitive to water.

Finally in this material testing study the flexural fatigue properties of these materials were examined. The fatigue results, normalized by quasi-static break load, are shown in Fig. 6.

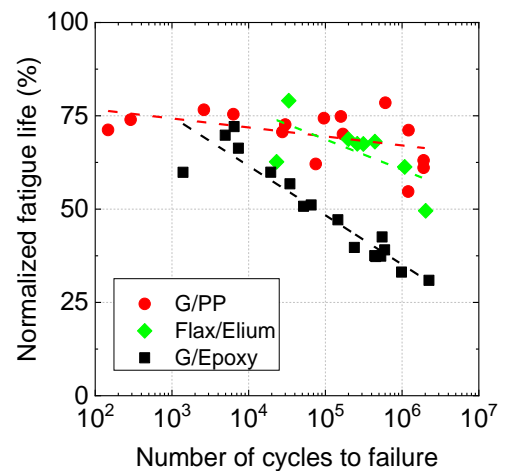
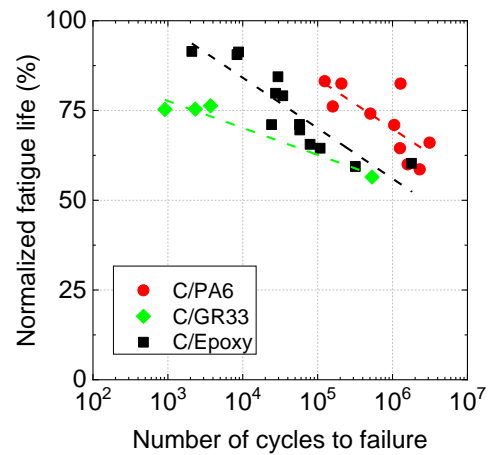
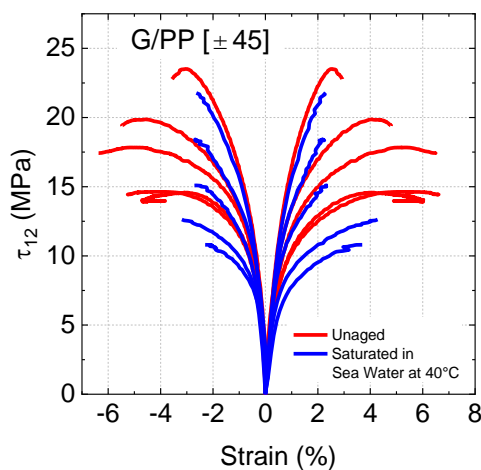
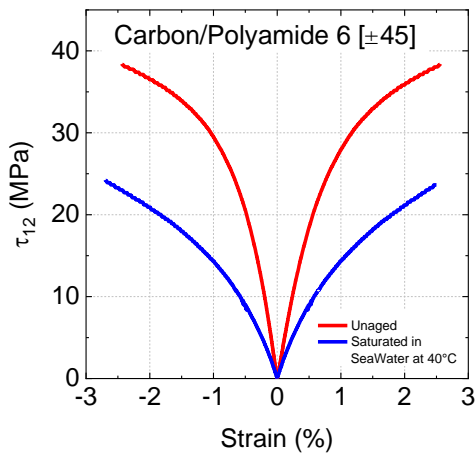


Fig. 6. Normalized S-N plots for all 6 materials.

These plots show the higher sensitivity of the glass/epoxy to fatigue, compared to the carbon reinforced composites, but the glass/PP shows much better performance than the glass/epoxy. After saturation all the alternative composites show a drop in lifetime but the performance of the glass/PP remains reasonably good, Fig. 7.

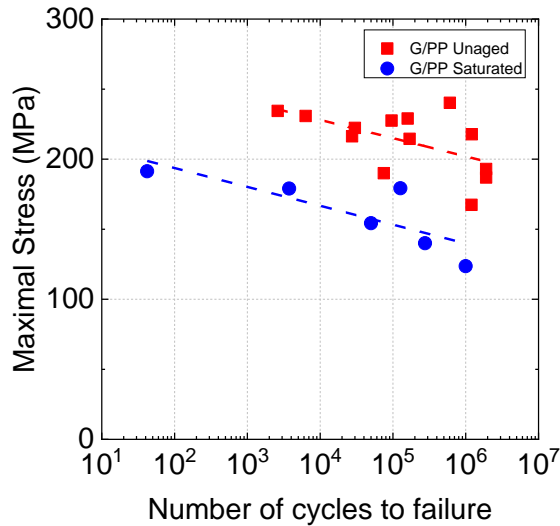


Fig. 7. S-N plots dry and after seawater saturation, glass/PP 0/90°.

Based on these data it is now possible to examine the influence of changing the material on the blade design. This can be done in a number of ways, from very simplified elastic analyses, such as the one which will be discussed here, through to full numerical simulation of the blade in its environment. The latter will be discussed in the following sections.

A first approach to material comparisons is simply to examine the measured stiffnesses of rectangular composite beams with uniformly distributed loading, dry and after seawater saturation, and compare the unidirectional composite materials in terms of their flexural stiffnesses. This assumes that blade stiffness is the main design criterion, which is clearly a very strong simplifying assumption.

A one meter wide five meter long cantilever beam geometry is examined, and the first design criterion is taken to be an equivalent end displacement to that of the carbon or glass reinforced reference materials. The deflection is proportional to the applied load and inversely proportional to the modulus. However, as the beam is loaded in flexure the deflection is proportional to the thickness cubed.

If we first compare the glass to the carbon reference materials the ratio of moduli (120 to 42 GPa) would require around 30% thicker glass laminates to achieve the same deflection. However, this comparison was examined in detail by Grogan *et al.* [2], who concluded, for the blade and loading conditions they studied, that glass fibre reinforced plastic alone was not a suitable

material for the main structural components of a large tidal turbine blade, due to higher strains (compared to CFRP) leading to failure. The influence of seawater on tensile strength shown in Figure 3b supports this conclusion.

For the carbon/PA6 and carbon/green epoxy the axial stiffnesses are quite similar to that of the reference, small differences being due to small differences in fibre contents. Changing material makes very little difference to the deflection, either in the dry or wet state, suggesting that both may be more environmentally friendly candidates. This is not the case for the alternative materials to the glass/epoxy. The glass/PP manufacturing route results in lower fibre content and a 25% lower modulus than the glass/epoxy, so it would need about around 10% higher thickness for the same deflection. The flax/acrylic tested here shows a significantly lower stiffness due to even lower fibre content, and would need around 40% more material for the same dry deflection as the glass/epoxy. To guarantee this deflection after seawater saturation would require roughly twice the dry glass thickness.

VI. BLADE TEST

While simple beam models can provide a first indication of the consequences of adopting alternative material the complex geometries of turbine blades impose the use of more realistic modelling. Finite Element (FE) models are widely employed, but it is first essential to validate the model experimentally. This is not straightforward. One approach is to strain gauge the blades of a prototype, Fig.8, and then record strains during tests at sea. This has been done within the RealTide project on the Sabella D10 turbine, Fig. 9.



Fig. 8. Strain gauge instrumentation of Sabella D10 tidal turbine blade. Installation of strain gauges on blade.



(b)

Fig. 9. Installation of data logger on Sabella turbine blade before immersion.

This has provided valuable information but in order to analyze the measured strain data the corresponding loading conditions (waves, current, turbulence) must also be known, and this requires extensive environmental monitoring. Special instrumentation to do this has been developed in previous studies [5], and further development is also part of the RealTide project [6], but these data were not available when testing started. It was therefore decided to design a specific test frame to provide data on blade response under carefully controlled conditions. This was the primary aim of this test but it also provided an opportunity to investigate a range of monitoring possibilities, as will be described below.

1) Test Frame Design

The first requirement was to determine representative test loading conditions. These were provided by Sabella and Bureau Veritas, and allowed a specific test frame to be designed, Fig. 10. Two hydraulic cylinders apply the loads through three loading points.

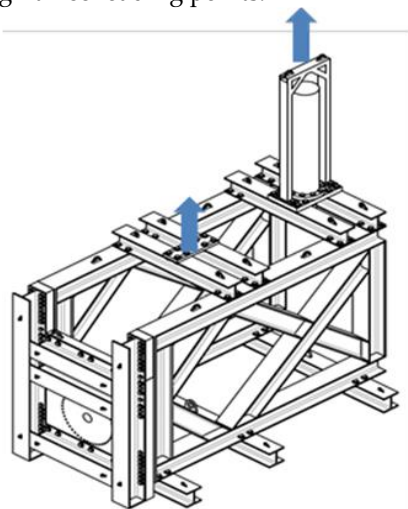
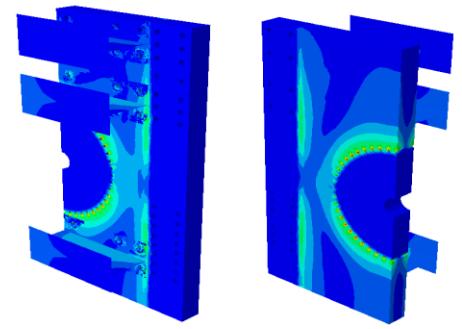
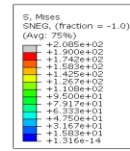
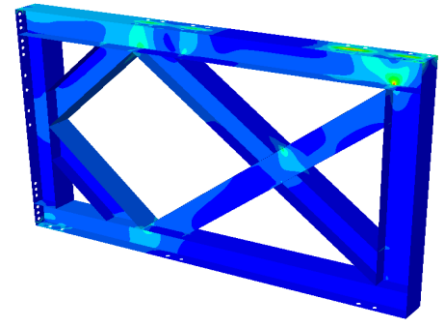
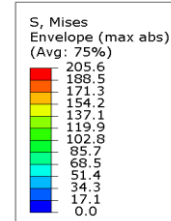


Fig.10. Schematic drawing of test frame

The critical components of this frame were studied in detail using FE models and Figure 11 shows two examples, for the plate to which the blade was fixed and the side of the frame.



(a)



(b)

Fig.11. FE models of test frame components, (a) fixing plate, (b) side wall frame.

2) Blade description and modelling

The blade which will be described here was 5 metres long. It was manufactured from mainly wet epoxy resin impregnated carbon fibres and contained 0° and $\pm 45^\circ$ carbon layers. Details of the construction are confidential but it consists of two skins of variable thickness and internal stiffeners. Figure 12 shows the blade being installed on the test frame.

It should be noted that this blade is not the Sabella D10 design, but a specific prototype developed within the RealTide project as a full scale platform to examine manufacturing parameters, modelling reliability and monitoring options.



Fig.12. Blade installation on the test frame.

The blade was modelled using ABAQUS™. Figure 13 shows the model together with an example of the predicted strains.

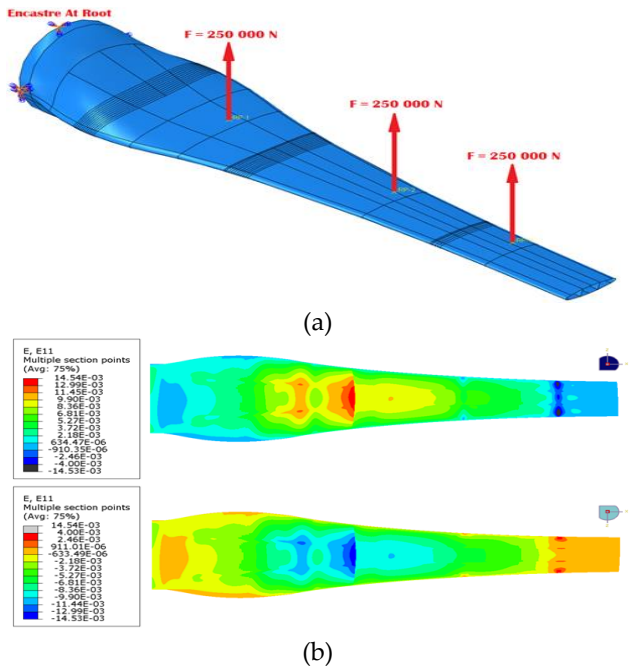
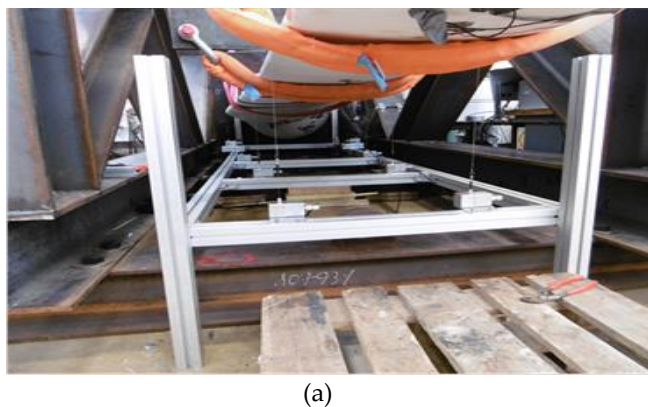


Fig. 13. FE model. (a) loading conditions, (b) example of predicted upper and lower surface strains.

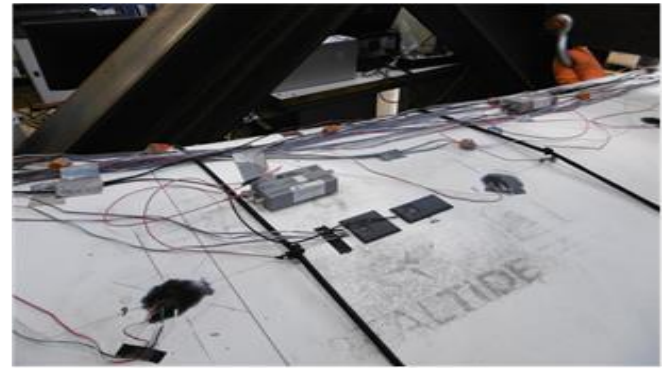
The results from this first model were used to optimize the instrumentation of the blade for the test, which was concentrated in the most highly loaded zone. This is the red region in Figure 14, and is the result of both the variable blade thickness and the presence of internal stiffeners.

3) Instrumentation

In order to measure the deflections a set of wire displacement transducers was installed on a frame below the blade, Fig. 14a. Strain gages rosettes were bonded every 500mm along the centre line. Two acoustic emission transducers were placed in the central section of the blade, Fig. 14b. Within the project, EnerOcean developed a novel ultrasonic wave propagation monitoring network with transducers along and inside the blade, also shown on Fig. 14b. Finally, two Luna Technology™ optical fibres [7], Fig. 15c, were installed within the blade skins during manufacture. These extended along the whole blade at the centre line and provided strains every 5 mm, the equivalent of 1000 strain gages.



(a)



(b)



(c)

Fig. 14. Blade instrumentation. (a) Displacement transducers, (b) Acoustic emission and EnerOcean transducers. (c) Blade tip showing optical fibre connections and interrogator box.

Table 2 summarizes the data channels and the five data acquisition systems used to record the measurements.

TABLE 2
DATA CHANNELS

Measurement (number)	Data Acquisition
Piston loads, displacements	Machine controller
Strain gages (46), Displacements (10)	HBM Logger
Acoustic emission (2)	EPA software & PC
Optical fibres (2)	Luna software & PC
EnerOcean gages (27), U/S (9)	Specific interface & software

In total around 100 data channels were recorded.

4) Examples of test results

Figure 15 shows the blade on the test frame and the three loading points.



Fig. 15. Blade on test frame during test.

A large number of tests were performed on the blade including a series of load-unload cycles, some sinusoidal cycling and finally a ramp to failure in January 2021. It is not possible to present results from all those tests here; but an example is shown below.

Fig. 16 shows one of the early loading cycles applied. These involved loading to a fixed value, 20 kN (2 tons) per loading point here (60 kN in all), holding for a short time then unloading at the same rate. At this load level no acoustic emission was recorded.

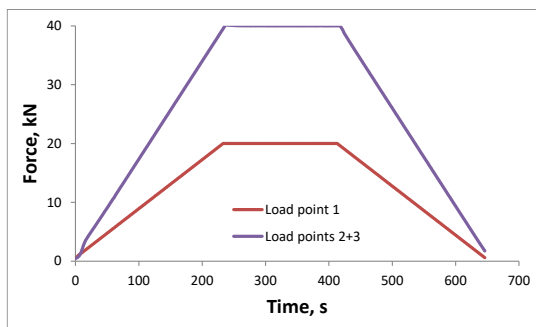


Fig. 16. Load-time recordings for load-unload test to 60 kN (20 kN per load point)

A first set of data is shown in Fig. 17, which presents the strain measurements recorded with an implanted optical fibre during load-unload tests up to 60 kN.

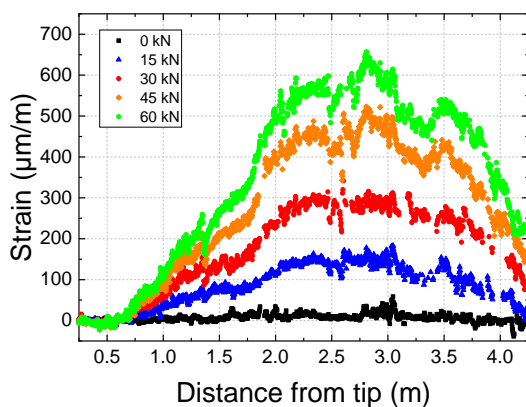


Fig. 17. Maximum surface microstrain measurements recorded with implanted optical fibre along the blade from tip (left) to root (right), during 5 loading tests to different levels up to 60 kN.

This instrumentation provides a full axial strain profile along the blade and indicates not only the highest strain regions, around the blade centre here, but also regions with strain gradients which may become failure locations.

VII. DISCUSSION

The development of this test facility allowing blades to be loaded under conditions which can simulate loading in service, has generated a large database of strain and displacement values. This has enabled FE models to be compared with real full scale test data and established confidence in the numerical simulation, e.g. Fig. 18. In this figure strains along the blade surface were predicted blind, using input data from coupon tests and nominal blade geometry and thicknesses. The form of the strain profile along the blade is predicted well. Predicted values are a little higher than measured strains but the blade thicknesses were a little higher than nominal values and this may explain the difference. Samples have been removed from the blade to check material properties.

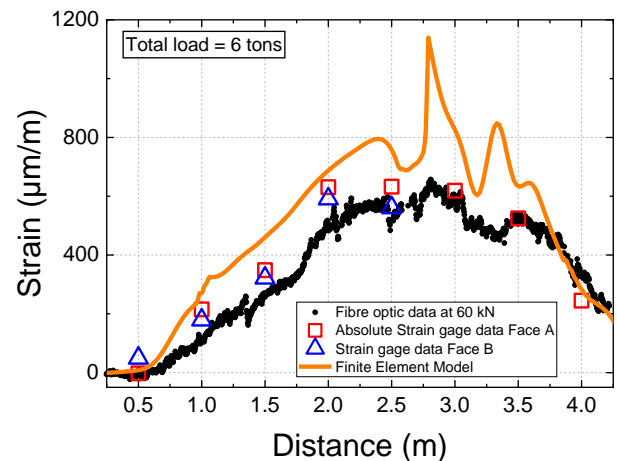


Fig. 18. Example of correlation between FE prediction of axial strains along blade and measured values from strain gages and optical fibre, plotted versus distance from blade tip, for an applied load of 60 kN.(20 kN at each loading point).

With a validated numerical model it is now possible to examine the influence of changing the material, based on the material property database generated within the RealTide project. This is currently underway.

VIII. CONCLUSIONS

First, a test frame specially designed to test 5 meter long tidal turbines has been constructed. A full scale blade has been instrumented with around 100 data points and tested. Traditional and innovative monitoring systems have been evaluated.

The blade was then cut into sections and specimens were analysed and test. This enabled the model input material properties to be checked, and the internal

damage mechanisms which led to final failure to be established. Based on this experience a second, improved blade was then manufactured and tested, and results from this second test will be published shortly.

ACKNOWLEDGEMENT

The authors are very grateful both to their many colleagues who participated in this work and also to all the partners of the RealTide project (Bureau Veritas, 1-Tech, EnerOcean, Ingeteam, Sabella, University of Edinburgh and IFREMER) for their support during this work.

REFERENCES

- [1] RealTide project website, <https://www.realtide.eu/>
- [2] D.M. Grogan, S.B. Leen, C.R. Kennedy, C.M. O'Bradaigh, Design of composite tidal turbine blades, 2013, Renewable Energy 57:151–162
<https://doi.org/10.1016/j.renene.2013.01.021>
- [3] A. LeDuigou, P. Davies, C. Baley, Environmental Impact Analysis of the Production of Flax Fibres to be Used as Composite Material Reinforcement, 2011, Journal of Biobased Materials and Bioenergy 5(1):153-165
<https://doi.org/10.1166/jbmb.2011.1116>
- [4] P. Davies, Towards More Representative Accelerated Aging of Marine Composites , 2020. In Lee S. (eds) Advances in Thick Section Composite and Sandwich Structures. Springer, pp.507-527.
<https://doi.org/10.1007/978-3-030-31065-3>
- [5] B. G. Sellar, D. R. J. Sutherland, D. M. Ingram and V. Venugopal, "Measuring waves and currents at the European marine energy centre tidal energy test site: Campaign specification, measurement methodologies and data exploitation," OCEANS 2017 - Aberdeen, pp. 1-7, doi: 10.1109/OCEANSE.2017.8085001.
- [6] C. Old et al., Deployment and Instrument Specification for Advanced Flow Characterisation, 2020, RealTide deliverable 2.1, available at:
https://www.realtide.eu/sites/realtide.eu/files/attachments/news/20190830/RealTide_Deliverable_2.1.pdf
- [7] M. Arhant, N. Meek, D. Penumadu, P. Davies, N. Garg, 2018, Residual Strains using Integrated Continuous Fiber Optic Sensing in Thermoplastic Composites and Structural Health Monitoring, . Experimental Mechanics , 58(1), 167-176
<https://doi.org/10.1007/s11340-017-0339-2>